ESTIMATION OF MULTIPLE LOCAL ORIENTATIONS IN IMAGE SIGNALS

Til Aach, Ingo Stuke

Institute for Signal Processing
University of Lübeck
Ratzeburger Allee 160, 23538 Lübeck
Germany

Cicero Mota, Erhardt Barth

Institute for Neuro- and Bioinformatics
University of Lübeck
Ratzeburger Allee 160, 23538 Lübeck
Germany

ABSTRACT

Local orientation estimation can be posed as the problem of finding the minimum grey level variance axis within a local neighbourhood. In 2D image signals, this corresponds to the eigensystem analysis of a 2×2-tensor, which yields valid results for single orientations. We describe extensions to multiple overlaid orientations, which may be caused by transparent objects, crossings, bifurcations, corners etc. Multiple orientation detection is based on the eigensystem analysis of an appropriately extended tensor, yielding so-called mixed orientation parameters. These mixed orientation parameters can be regarded as another tensor built from the sought individual orientation parameters. We show how the mixed orientation tensor can be decomposed into the individual orientations by finding the roots of a polynomial. Applications are, e.g., in directional filtering and interpolation, feature extraction for corners or crossings, and signal separation.

1. INTRODUCTION

Estimation of local orientation is essential in a variety of multidimensional signal filtering and analysis tasks, like directional filtering [1, 2], directional interpolation [3], feature extraction for pattern analysis [4, 5], and the concept of intrinsic dimension [6]. Local orientation can be defined as the direction along which the grey level profile exhibits least average variation over a small neighbourhood. The orientation can then be found by analysing the eigenvectors of a tensor, while the grey level variation along and perpendicular to the orientation is given by the lower and larger eigenvalue, respectively. The elements of the tensor are calculated from the observed image data by filtering, viz. by differentiation or by quadrature filters, and nonlinear operations like squaring [4, 7, 5, 8]. This framework assumes that only a single orientation is present. In case of two or more superimposed orientations, the eigenvectors no longer represent orientation. Such neighbourhoods — generated,

for instance, by corners — are characterized by the lower eigenvalue being reasonably large, indicating that no axis along which the grey level variation is low can be found.

Multiple orientations are caused by non-opaque structured objects, e.g. in X-ray imaging, or by bifurcations, corners, crossings, etc. Multiple orientations are also ubiquitous in Radon space, when sine curves of different objects cross. We describe an approach for the simultaneous estimation of multiple local orientations. Our problem formulation is based on a comparable approach to estimating multiple optic flows [9, 10], which can be viewed as 3D-orientations in space and time. We will show that multiple orientations can be estimated by the eigensystem analysis of a suitably extended tensor, yielding so-called mixed orientation parameters. For the case of double orientation, we separate the mixed orientation parameters into the individual orientations by analytically finding the roots of a second degree polynomial (cf. [10, 11]).

2. ORIENTATION ESTIMATION

We briefly review the estimation of a single orientation in a bivariate signal $f(\mathbf{x})$, $\mathbf{x}^T = (x, y)$, characterized by an angle θ with respect to the horizontal axis [7, 4]. Let

$$\alpha(\phi) = \cos(\phi)\partial_x + \sin(\phi)\partial_y, \ \ \partial_x = \frac{\partial}{\partial x}, \ \ \partial_y = \frac{\partial}{\partial y} \ \ (1)$$

denote the differential operator in the direction ϕ. If $f(x, y)$ is ideally oriented at (x, y), its derivative in the direction of θ is zero, i.e.

$$\alpha(\theta)f(\mathbf{x}) = \mathbf{v}^T \nabla f = 0, \ \ \mathbf{v}^T = (\cos\theta, \sin\theta) = \mathbf{v}^T(\theta) \tag{2}$$

Excluding the case of a (locally) constant signal, this is a necessary and sufficient condition, which, when met for θ, is also met for $\theta \pm \pi$. We therefore restrict θ to lie within $(-\pi/2, \pi/2]$. Practically, local orientation is evaluated over a local neighbourhood Ω, within which it is assumed to be

constant. Minimizing the square error of condition (2) with respect to the angle yields

$$\theta = \min_\phi Q(\phi) = \min_\phi \left\{ \int_\Omega \left(\mathbf{v}(\phi)^T \nabla f \right)^2 d\Omega \right\}$$
$$\text{with } \mathbf{v}^T \mathbf{v} = 1 \quad (3)$$

$Q(\phi)$ is a measure of the variation of $f(\mathbf{x})$ in the direction ϕ. (In practice, the integrand in eq. (3) is often weighted by a function $w(\mathbf{x})$ emphasizing the central pixels in Ω, and with a continuous roll-off towards its borders. Since this weighting does not influence our considerations, we drop it for ease of notation.) $Q(\phi)$ can be rewritten to

$$Q(\phi) = \mathbf{v}^T \mathbf{T} \mathbf{v}, \quad \mathbf{v}^T \mathbf{v} = 1 \quad (4)$$

with the 2×2 tensor $\mathbf{T}$ being given by the tensor product

$$\mathbf{T} = \int_\Omega \nabla f \, (\nabla f)^T \, d\Omega = \int_\Omega \begin{bmatrix} f_x^2 & f_x f_y \\ f_x f_y & f_y^2 \end{bmatrix} d\Omega$$
$$= \int_\Omega \nabla f \otimes \nabla f d\Omega \quad (5)$$

Minimizing the composite criterion

$$L(\mathbf{v}) = \mathbf{v}^T \mathbf{T} \mathbf{v} + \lambda(\mathbf{v}^T \mathbf{v} - 1) \quad (6)$$

is equivalent to finding $\mathbf{v}$ such that

$$\mathbf{T} \mathbf{v} = \lambda \mathbf{v} \text{ with } \mathbf{v}^T \mathbf{v} = 1 \quad (7)$$

i.e. finding the normalized eigenvector of $\mathbf{T}$ corresponding to the lower eigenvalue λ. Note that $\mathbf{v}(\theta)$ is then uniquely determined up to a sign, which in turn is determined by the constraint $\theta \in (-\pi/2, \pi/2]$. The minimum average variation of $f(\mathbf{x})$ over Ω then is

$$Q(\theta) = \mathbf{v}^T \mathbf{T} \mathbf{v} = \mathbf{v}^T \lambda \mathbf{v} = \lambda \quad (8)$$

If $f(\mathbf{x})$ is ideally oriented in Ω, we have

$$\alpha(\theta) f(\mathbf{x}) = 0 \quad \forall \mathbf{x} \in \Omega \quad (9)$$

and thus $\lambda = 0$, or rank$(\mathbf{T}) = 1$. Denoting the Fourier transform of $f(\mathbf{x})$ taken over Ω by $F(\omega)$, where $\omega = (\omega_x, \omega_y)^T$, (9) becomes in the spectral domain

$$\mathbf{v}^T(\theta) \omega F(\omega) = 0 \quad (10)$$

i.e. $F(\omega)$ must be zero everywhere except on the line $\mathbf{v}^T \omega = 0$. $F(\omega)$ then is a Dirac distribution along $\mathbf{v}^T \omega = 0$.

3. MULTIPLE ORIENTATION ESTIMATION

Let us now assume a signal $f(\mathbf{x})$ being composed from N oriented and non-opaque subsignals $f_i(\mathbf{x})$, $i = 1, \ldots N$, according to

$$f(\mathbf{x}) = \sum_{i=1}^N f_i(\mathbf{x}), \text{ with } \alpha(\theta_i) f_i(\mathbf{x}) = 0 \ \forall \mathbf{x} \in \Omega \quad (11)$$

where θ_i is the orientation of f_i. Excluding the case of one or more subsignals being constant, we have

$$f(\mathbf{x}) = \sum_{i=1}^N f_i(\mathbf{x}), \text{ with } \alpha(\theta_i) f_i(\mathbf{x}) = 0$$
$$\Leftrightarrow \alpha(\theta_N) \ldots \alpha(\theta_1) f(\mathbf{x}) = 0 \quad (12)$$

With $F_i(\omega)$ denoting the Fourier transform of $f_i(\mathbf{x})$ over Ω, and $\mathbf{v}_i^T = (\cos \theta_i, \sin \theta_i)$, we obtain in the spectral domain

$$\alpha(\theta_N) \ldots \alpha(\theta_1) f(\mathbf{x}) = 0 \circ\!\!-\!\!\bullet \ F(\omega) \cdot \prod_{i=1}^N (\mathbf{v}_i^T \omega) = 0 \ (13)$$

that is, the local spectrum $F(\omega)$ of $f(\mathbf{x})$ must be zero except over the lines $\mathbf{v}_i^T \omega = 0$.

For the case of two subsignals, we have $N = 2$, and this framework becomes

$$f(\mathbf{x}) = f_1(\mathbf{x}) + f_2(\mathbf{x}), \ \alpha(\theta_1) f_1(\mathbf{x}) = \alpha(\theta_2) f_2(\mathbf{x}) = 0$$
$$\Leftrightarrow \alpha(\theta_2) \alpha(\theta_1) f(\mathbf{x}) = 0 \quad (14)$$

We rewrite the lower row as the inner product $\mathbf{a}^T \mathbf{d} f = 0$, where

$$\mathbf{a}^T = (a, b, c) = (\cos \theta_1 \cos \theta_2, \sin(\theta_1 + \theta_2), \sin \theta_1 \sin \theta_2) \quad (15)$$

and

$$\mathbf{d} f = (f_{xx}, f_{xy}, f_{yy})^T \quad (16)$$

The components of the vector $\mathbf{a}$ are the so-called mixed orientation parameters formed from the orientation vector components $\mathbf{v}_i = (\cos \theta_i, \sin \theta_i)$, $i = 1, 2$. In the following, we first solve for the mixed orientation vector $\mathbf{a}$, and then decompose it into $\mathbf{v}_1$ and $\mathbf{v}_2$.

We seek $\mathbf{a}$ — and thus the orientation angles θ_1 and θ_2 — such that the summed square error

$$Q(\mathbf{a}) = \int_\Omega (\alpha(\theta_1) \alpha(\theta_2) f(\mathbf{x}))^2 \, d\Omega = \int_\Omega (\mathbf{a}^T \mathbf{d} f)^2 d\Omega \quad (17)$$

evaluated over Ω is minimized. To exclude the trivial solution, we impose the constraint $\mathbf{a}^T \mathbf{a} = R$, with $R > 0$ (the precise value of R plays no role in the following discussion). The minimization functional then becomes

$$L(\mathbf{a}) = \mathbf{a}^T \mathbf{T}_2 \mathbf{a} + \lambda(\mathbf{a}^T \mathbf{a} - R) \quad (18)$$

where the tensor $\mathbf{T}_2$ is computed from the observed image signal by

$$\mathbf{T}_2 = \int_\Omega \begin{bmatrix} f_{xx}^2 & f_{xx} f_{xy} & f_{xx} f_{yy} \\ f_{xy} f_{xx} & f_{xy}^2 & f_{xy} f_{yy} \\ f_{xx} f_{yy} & f_{xy} f_{yy} & f_{yy}^2 \end{bmatrix} d\Omega$$
$$= \int_\Omega \mathbf{d} f \otimes \mathbf{d} f d\Omega \quad (19)$$

The solution then is

$$\mathbf{T}_2 \mathbf{a} = \lambda \mathbf{a} \quad \text{with} \quad \mathbf{a}^T \mathbf{a} = R \qquad (20)$$

where $\mathbf{a}$ is the eigenvector corresponding to the lowest eigenvalue λ of $\mathbf{T}_2$. In the case of two ideal orientations, $\mathbf{T}_2$ is of rank two, and $\lambda = 0$.

The mixed orientation vector $\mathbf{a}$ can be regarded as a full — albeit implicit — description of the two orientations in the neighbourhood Ω. This description could be used as a corner feature for, e.g., corner tracking. Explicit multiple orientation analysis, however, requires decomposition of $\mathbf{a}$ into the sought orientations θ_1 and θ_2. Here, we describe an analytical and numerically very stable method. Let

$$\mathbf{v}_i^T = (\cos\theta_i, \sin\theta_i) = (v_i^x, v_i^y) \qquad (21)$$

for $i = 1, 2$. Eq. (15) then becomes

$$\mathbf{a}^T = (a, b, c) = (v_1^x v_2^x, v_1^x v_2^y + v_1^y v_2^x, v_1^y v_2^y) \qquad (22)$$

Building a 2×2-matrix $\mathbf{M}$ according to

$$\mathbf{M} = \begin{bmatrix} v_1^x v_2^x & v_1^x v_2^y \\ v_1^y v_2^x & v_1^y v_2^y \end{bmatrix} = \begin{bmatrix} a & z_1 \\ z_2 & c \end{bmatrix} \qquad (23)$$

we see that its first and second row encode θ_2 by $v_1^x \mathbf{v}_2^T$ and $v_1^y \mathbf{v}_2^T$, respectively, while its columns specify θ_1 by $v_2^x \mathbf{v}_1$ and $v_2^y \mathbf{v}_1$. The elements on the main diagonal of $\mathbf{M}$ are directly given by $\mathbf{a}$. The elements z_1 and z_2 on the counter diagonal can be found as follows: First, observe that $z_1 z_2 = ac$, and $z_1 + z_2 = b$. Therefore, z_1 and z_2 are simply the roots of the polynomial

$$P(z) = (z - z_1)(z - z_2) = z^2 - bz + ac \qquad (24)$$

which is fully specified by the mixed orientation vector $\mathbf{a}$. Since $\mathbf{v}_i^T \mathbf{v}_i = 1$, $i = 1, 2$,

$$\mathbf{v}_2 = \frac{(a, z_1)^T}{\sqrt{a^2 + z_1^2}} = \frac{(z_2, c)^T}{\sqrt{z_2^2 + c^2}} \qquad (25)$$

and similarly for $\mathbf{v}_1$. The angle θ_2 then is

$$\theta_2 = \arctan\left(\frac{z_1}{a}\right) = \arctan\left(\frac{c}{z_2}\right) \qquad (26)$$

which lies in $(-\pi/2, \pi/2]$. Alternatively, one might wish to use both rows of $\mathbf{M}$ for increased robustness and numerical stability. Denoting the first and second row of $\mathbf{M}$ by $\mathbf{l}_1^T$ and $\mathbf{l}_2^T$, respectively, we find for $\mathbf{v}_2$

$$\mathbf{v}_2 = \frac{||\mathbf{l}_1||\mathbf{l}_1 + ||\mathbf{l}_2||\mathbf{l}_2}{||\mathbf{l}_1||^2 + ||\mathbf{l}_2||^2} \qquad (27)$$

if $\mathbf{l}_1^T \mathbf{l}_2 \geq 0$, and

$$\mathbf{v}_2 = \frac{||\mathbf{l}_1||\mathbf{l}_1 - ||\mathbf{l}_2||\mathbf{l}_2}{||\mathbf{l}_1||^2 + ||\mathbf{l}_2||^2} \qquad (28)$$

otherwise. To find $\mathbf{v}_1$, we replace in these expressions the rows of $\mathbf{M}$ by its columns.

4. RESULTS

Fig. 1 shows two oriented patterns $f_1(\mathbf{x})$ and $f_2(\mathbf{x})$ superimposed to form the image $f(\mathbf{x}) = f_1(\mathbf{x}) + f_2(\mathbf{x})$, and the orientations estimated by our algorithm. For reasons of clarity, the orientations are represented by sparse vector maps. The discrete approximations to the derivatives were calculated by the 3×3 Prewitt filter kernels, and the integration over Ω was realized as a 5×5 moving average. The good agreement between true and estimated orientations is already visually evident. A more quantitative assessment of the estimation accuracy is possible by calculating $\alpha(\theta_1)f(\mathbf{x})$, where θ_1 is the estimate of the orientation of $f_1(\mathbf{x})$. If this estimate is correct, $\alpha(\theta_1)f(\mathbf{x}) = 0$, i.e. $f_1(\mathbf{x})$ is "nulled" out. Thus, $\alpha(\theta_1)f(\mathbf{x}) = \alpha(\theta_1)f_2(\mathbf{x})$. This residual is a linear filtered version of $f_2(\mathbf{x})$, which must have the same orientation as $f_2(\mathbf{x})$. Examining the left-hand side of Fig. 2 shows that indeed only a pattern with orientation $-\pi/4$ remains. The converse is shown on the right-hand side for $\alpha(\theta_2)f(\mathbf{x})$. Apart from orientation estimation, the framework hence also allows to separate the detected oriented patterns modulo a convolution.

For a more detailed error analysis, we changed the orientations of the patterns in Fig. 1 in steps of 10 degrees, and measured the root mean square error of the estimated angles for each pair of orientations. Fig. 3 shows the measured RMSE in degrees over orientations. The RMSE is lowest when the orientations are aligned with the image grid (0, 45 and 90 degrees), and largest in between. It is hence obviously dominated by sampling effects rather than by the angular differences of the orientations. Even in the worst case, the maximum RMS error is less than 4 degrees.
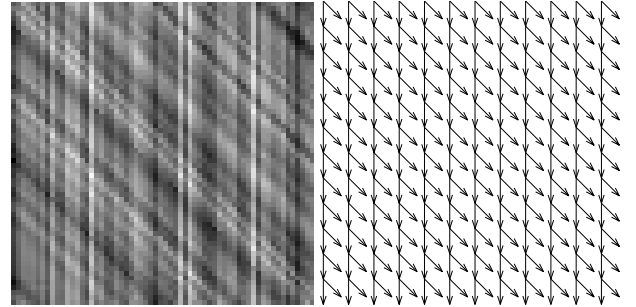

Fig. 1. Left: Synthetic image of size 62×62 pixels with two superimposed orientations of $\pi/2$ and $-\pi/4$. Right: Estimated orientations represented by vectors.

5. DISCUSSION

We have described a two-step approach towards estimating multiple overlaid orientations. First, we estimate a mixed orientation vector by analysing the eigensystem of a tensor.
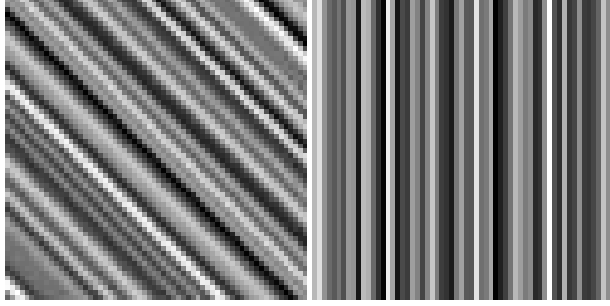
Fig. 2. Results of "nulling" by $\alpha(\theta_1)f(\mathbf{x})$ (left) and $\alpha(\theta_2)f(\mathbf{x})$ (right). For details see text.
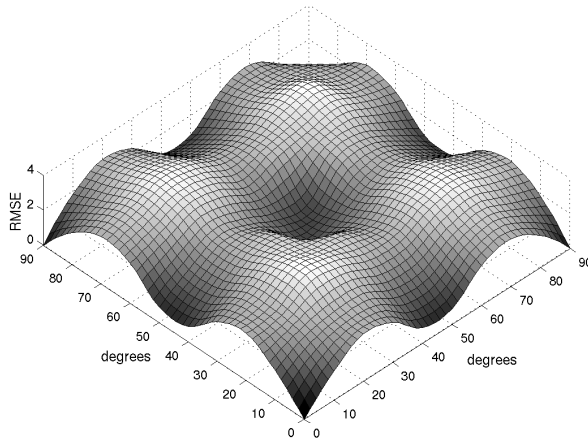
Fig. 3. Root mean square error of estimated angles over true angle pairs. For better visualization, the error surface is interpolated between the measurements.

The mixed orientation vector is then decomposed into the sought orientations by finding the roots of a polynomial. For ease of notation and because of limited space, we focussed on two overlaid orientations in two dimensions. While the tensor eigensystem in Eqs. (19) and (20) can straightfor-wardly be generalized towards both more orientations and more dimensions, the separation will become considerably more complex unless one restricts oneself to either two dimensions with three or more orientations, or to two orientations in three or more dimensions.

As in the single orientation case, where the involved 2×2-tensor $\mathbf{T}$ is of rank 1 when indeed only a single orientation is present, the 3×3-tensor $\mathbf{T}_2$ in eq. (19) for the double orientation case is rank deficient ($\mathrm{rank}(\mathbf{T}_2) = 2$) when indeed only two orientations exist. The eigenvalues of the corresponding tensor can therefore be used as a measure of confidence for the number of orientations tested, and hierarchical algorithms testing successively for one, two or

more orientations be derived.

Our experiments show that even simple gradient filters perform reasonably well, nonetheless we intend to evaluate the estimation accuracy and noise resistance of other, optimized gradient filters, like [12, 13] in the near future. Another topic for future research efforts is regularization of the mixed orientation parameters (cf. for motion [14]). Finally, our framework can also be extended towards multispectral images, based on the tensor defined in [15] for describing gradients in, e.g., color images.

6. REFERENCES

[1] T. Aach, D. Kunz, "Anisotropic spectral magnitude estimation filters for noise reduction and image enhancement," *Proc. IEEE ICIP-96*, Lausanne, Sept 16–19 1996, 335–338.

[2] T. Aach, D. Kunz, "A lapped directional transform for spectral image analysis and its application to restoration and enhancement," *Signal Processing* 80(11):2347–2364, 2000.

[3] J. Hladuvka, E. Gröller, "Direction-driven shape-based interpolation of volume data," in *Proc. Vision, Modeling, Visualization*, Stuttgart, Nov 21–23 2001, 113–120, 521.

[4] M. Kass, A. Witkin, "Analyzing oriented patterns," *Comp. Vis. Graph. Im. Proc.* 37:362–385, 1987.

[5] H. Knutsson, G. H. Granlund, "Texture analysis using two-dimensional quadrature filters," *IEEE Works. Comp. Arch. Patt. Anal. Im. Data Base Manag.*, Pasadena, Oct 1983.

[6] C. Zetzsche, E. Barth, "Fundamental limits of linear filters in the visual processing of two-dimensional signals," *Vision Research* 30:1111–1117, 1990.

[7] J. Bigün, G. H. Granlund, "Optimal orientation detection of linear symmetry," in *Proc. IEEE 1st Intl. Conf. Comp. Vis.*, London, June 1987, 433–438.

[8] G. H. Granlund, H. Knutsson, *Signal Processing for Computer Vision*, Kluwer, Dordrecht, 1995.

[9] M. Shizawa, K. Mase, "Simultaneous multiple optical flow estimation," *Proc. IEEE Intl. Conf. Comp. Vis. Patt. Recog.*, Atlantic City, June 1990, 274–278.

[10] C. Mota, I. Stuke, E. Barth, "Analytic solutions for multiple motions," *Proc. IEEE ICIP, Vol. II*, Thessaloniki, Oct 7–10 2001, 917–920.

[11] E. Barth, I. Stuke, C. Mota, "Analysis of motion and curvature in image sequences," *5th IEEE Southwest Symp. Im. Anal. Interpr.*, Santa Fe, April 7 - 9 2002, 206–210.

[12] H. Scharr, B. Jähne, "Optimization of spatio-temporal filter families for fast and accurate motion estimation," *Im. Seq. Anal. to Investi. Dyn. Proc., Lecture Notes in Computer Science*. 2003, Springer.

[13] M. Elad, P. Teo, Y. Hel-Or, "On the design of optimal filters for gradient-based motion," *Intl. Journ. Comp. Vis.* (submitted), 2002.

[14] I. Stuke, T. Aach, C. Mota, E. Barth, "Linear and regularized solutions for multiple motions," *IEEE ICASSP 2003*, Hong Kong, April 6–10 2003, III 157–160.

[15] S. Di Zenzo, "A note on the gradient of a multi-image," *Comp. Vis. Graph. Im. Proc.* 33:116–125, 1986.